 Revista Mexicana de Física **40**, *No. 3 (1994) 418–426*

Structure and composition of CdSbTe thin films grown by radio frequency sputtering

O. ALVAREZ-FREGOSO
Instituto de Investigación en Materiales
Universidad Nacional Autónoma de México
México, D.F., México

F. SÁNCHEZ-SINENCIO, J.G. MENDOZA-ALVAREZ, O. ZELAYA
Departamento de Física
Centro de Investigación y Estudios Avanzados del IPN
México, D.F., México

M.H. FARÍAS, L. COTA-ARAIZA AND G.SOTO
Laboratorio de Ensenada, Instituto de Física
Universidad Nacional Autónoma de México
Ensenada, B.C., México

Recibido el 26 de julio de 1993; aceptado el 30 de noviembre de 1993

ABSTRACT. Cadmium antimonide telluride thin films with Sb concentrations, x, in the range 8–60 at% were grown onto glass substrates by an r.f. sputtering deposition technique at substrates temperatures of $\sim$ 50 °C. Film composition was measured by an Auger electron spectroscopy (AES) system, and from a depth profiling analysis in the samples monitoring the Cd, Te and Sb AES lines, we found an amphoteric behavior of Sb with nearly equal chances of substituting either Cd or Te in the CdTe lattice. Sample structure was studied by X-ray diffraction (XRD), having found the presence of the cubic phase resembling the CdTe XRD pattern with a preferential growth along the (111) direction, for low Sb concentrations. The main effect of Sb in the lattice was the amorphization of the structure for films with $x \geq 0.30$. We also present the results for the electrical resistivity dependence on x, as well as the behavior of the activation energy for the CdSbTe films with different Sb content.

RESUMEN. Películas delgadas de cadmio-antimonio-telurio con concentraciones, x, en el intervalo 8–60 (% at) fueron crecidas sobre substratos de vidrio por *sputtering* de radio frecuencia a temperaturas de substratos de $\sim$ 50 °C. La composición de las películas se determinó por espectroscopía de electrones Auger (AES). De un análisis del perfil de profundidad en las muestras, midiendo las líneas AES del Cd, Te y Sb, encontramos un comportamiento anfotérico del Sb, con aproximadamente igual probabilidad de sustituir al Cd o al Te de la red del CdTe. La estructura de las películas fue estudiada por difracción de rayos X (XRD), habiéndose encontrado la presencia de la fase cúbica semejante al patrón XRD del CdTe con una orientación preferencial en la dirección (111), para bajas concentraciones de Sb. El principal efecto del Sb en la red consistió en la amorfización de la estructura para películas con $x \geq 0.30$. Presentamos resultados de la dependencia de la resistividad con x, así como también de la energía de activación para las películas de CdSbTe con diferente contenido de Sb.

PACS: 61.42.Th; 73.60.Cs

1. Introduction

Ternary and pseudo-binary alloys are currently being investigated due to their electro-optical properties that make them particularly suitable for optical, acoustic, electro-optic, and electronic devices. The crystalline structure for this type of compounds is normally derived from the diamond-like structure modified to accommodate three or more atoms of different sizes which allow additional symmetries resulting in crystals with larger refractive indices, and bandgap energies running from narrow (< 1 eV) to wide (> 3 eV) gaps allowing optical transmission ranges from UV through visible to the near infrared. These properties have been used in the development of devices such as acousto-optic and electro-optic modulators, switches, optical filters, frequency doublers, and photovoltaic solar cells [1–5].

Thin film growth of ternary and pseudo-binary alloys can be achieved by different methods; in particular, the radio frequency (r.f.) sputtering deposition technique offers the possibility of a wide range control of compositions, and an extensive investigation of their structural, optical and electrical properties is required for any practical applications.

In this paper, we report the method and deposition parameters for the growth of CdSbTe films with Sb concentrations in the range from 0 to 60 at% as determined by Auger electron spectroscopy (AES) analysis, and the characterization of their structural and electrical properties as a function of the antimony concentrations in the film.

2. Experimental

The CdSbTe films were grown in a diode r.f. sputtering system with a CdTe target with 5 cm^2 in area (A) placed on a water-cooled cathode. The target used as the source for the sputtering process was made by vacuum pressing 99.999% pure CdTe powder, adding in the top a piece of antimony with a variable area $A_i = (0.016, 0.04, 0.078, 0.15, 0.18,$ and $0.25)$ A. As substrates we used 7059 Corning Glass slides. Separation between target and substrate was around 3 cm. The sputtering system was preevacuated to $\sim 5 \times 10^{-6}$ Torr and then flushed through with purified Argon gas for at least 15 min, at a working pressure of 5 mTorr, before the plasma was initiated. The target was usually presputtered under growth conditions for 15 min just before deposition. The samples were growth under the following typical conditions: Background pressure $= 5 \times 10^{-6}$ Torr; Ar pressure = 5 mTorr; r.f. power = 100 watts; deposition time = 120 min; and substrate temperature $\simeq 50$ °C.

Film thicknesses were determined by an interferometric method on test samples, and was usually in the range: 0.2–0.3 μm. The film antimony concentration obtained when the different targets of area A_i were used, was measured using a scanning Auger microscopy-electron spectroscopy for chemical analysis (PHI560/ESCA-SAM) system. The electron gun was operated at 3 keV and beam currents were kept around 2.5 μA. Auger data were recorded after cleaning the surface from contaminants by using a 2 keV argon ion beam with a diameter of around 0.4 mm, which gives a current density on the sample of 12 $\mu A/cm^2$. The film crystalline structure was studied through the XRD patterns using an X-ray diffractometer Siemens D500 (CuK_α).

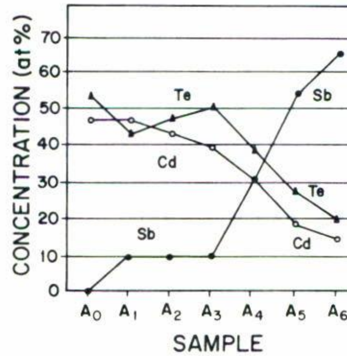

FIGURE 1. Percentages of Cd, Te and Sb in the CdSbTe thin films as measured by AES analysis. Sample A_0 corresponds to a pure CdTe film. Note that the Cd concentration decreases slightly more than the Te does, as the Sb concentration increases.

Resistivity measurements were performed at room temperature ($\sim$ 300 °K) using a two-electrode method [6]. Samples of 0.5×0.5 cm^2 with gold coplanar electrodes were used in the resistivity experiments. Special care was taken in the measurement of the electrical conductivity as a function of temperature in order to minimize any possible annealing effect at high temperatures (100–150 °C) on the A_4, A_5 and A_6 amorphous samples.

3. Results and discussion

3.1. *Thin film composition*

The CdSbTe film composition was determined by Auger electron spectroscoy (AES). Auger survey of films exposed to air showed Cl, C, O, and S as the main surface contaminants. Argon ion bombardment for a short time was necessary in order to get a clean surface spectrum. The Auger measurement took into account the Auger sensitivity for the peak-to-peak height ratio between the Cd and Te signals. Here, we used a 1.17:1 ratio for the Cd:Te intensities of stoichiometric CdTe which was obtained from the best fit of our measurements, and is in good agreement with the existing literature [7,8].

Figure 1 shows the film composition in terms of the Cd, Te and Sb percentages for the different A_i's samples. A_0 indicates a zero Sb content; $A_1 = (0.016)A$ for target top surface covered with Sb, etc. As it can be observed in Fig. 1, both the Cd and Te concentrations decreases as the Sb content increases; this is a possible indication of the amphoteric character of antimony in the CdTe lattice at the Cd and Te sites. AES accurate analysis by scanning profile showed that the films were homogeneous and free of antimony clusters [7,9].

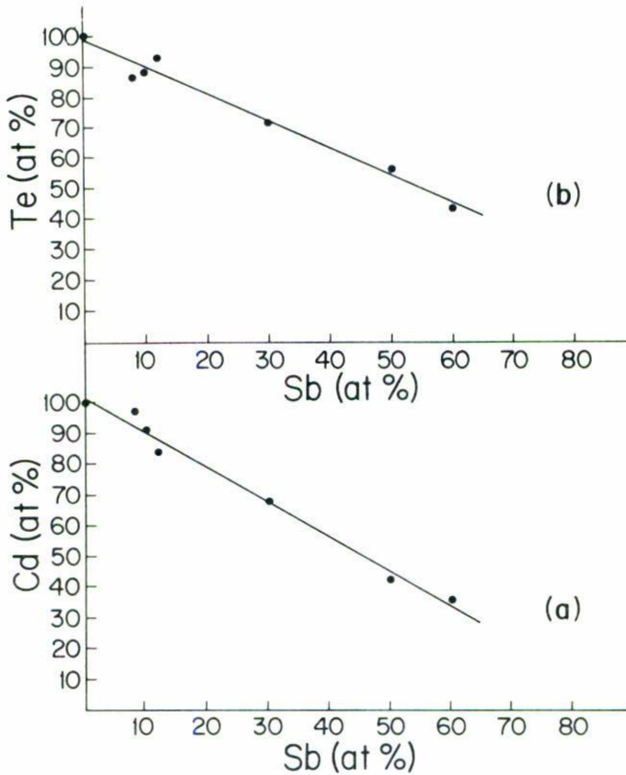

FIGURE 2. Functional relationship between the Sb concentration and, a) Cd concentration; b) Te concentration. Note that there exists an almost linear dependence in both figures with a slope very close to one.

The functional relationships between the cadmium and tellurium percentages respect to the antimony percentage are shown in Figs. 2a and 2b. As can be observed in those plots, the function is linear in both figures with an almost ideal slope ($m \approx 1$), indicating that the Sb atoms have almost equal chance in substituting to Cd or Te sites in nearly equal quantities; this fact is represented by means of the chemical formula: $Cd_{1-x/2}Sb_xTe_{1-x/2}$ with $x =$ at% of antimony as determined by AES.

3.2. Dependence of structure on Sb concentration

X-ray diffractometry was used to determine the crystallinity, structure, and grain size of the films. In Fig. 3 we show the X-ray diffraction patterns (XRD) for the CdSbTe thin films grown with different Sb concentrations. In this figure the A_0(XRD) pattern corresponds to a pure CdTe film. Scattering geometry allows us to detect only those planes parallel to the substrate. The film is polycrystalline and has a cubic (zincblende) structure with a strong (111) texture. The XRD patterns for the A_1, A_2 and A_3 samples, corresponding to Sb concentrations of 8, 10 and 12%, respectively, resemble the A_0 pattern for CdTe showing also an intense (111) preferential orientation. The presence of the cubic phase throughout the range $0 \leq x \leq 0.12$ of Sb concentration agrees with the trend observed for other II-VI-based thin film compounds [10,11], but it disagrees with the results and

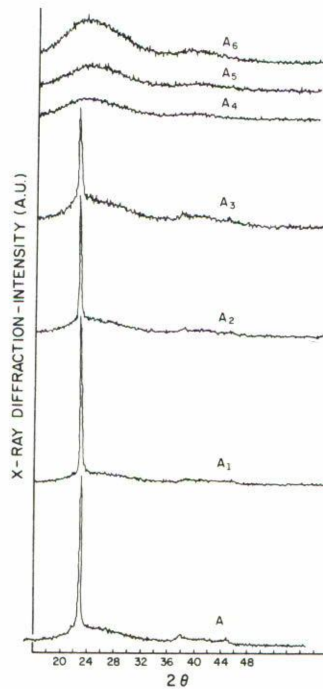

FIGURE 3. X-ray diffraction patterns for the films A_0 through A_6. Films A_0 to A_3 show the presence of the cubic structure with a strong (111) texture; whereas for films A_4 to A_6 the amorphous phase is observed.

observations of mixtures of the hexagonal and cubic phases reported for CdTe and CdFeTe thin films grown by several methods [12–15]. At this time, it is not possible for us to say conclusively that no hexagonal phase is present in our CdSbTe films, due to the very close registry of the two patterns and the very strong (111) texture.

In Table I we present the calculated lattice parameters based on the cubic indexing. From the ASTM X-ray powder data file (cards nos. 15–770 and 19–193) is clear that the CdTe film has a slightly larger lattice parameter than the one corresponding to the monocrystal and powder sample ($a = 6.481$ Å). This result could be due to an internal stress effect and the polycrystalline character for the film. Lattice parameters for the A_1, A_2 and A_3 samples are 0.2, 0.21 and 0.26 % larger than the value for the A_0 sample; this last result can be understood because of the larger size of the Sb atom as compared to the Cd and Te atoms that results in a lattice expansion when the Sb enters in the Cd and Te sites (Sb: 2.45 Å, Te: 2.21 Å, Cd: 0.97 Å; ionic radios).

From the FWHI of the X-ray diffraction peak, we estimated the film grain size [16] obtaining values between 200–300 Å for the A_0, A_1, A_2 and A_3 samples. The films A_4, A_5 and A_6 show an amorphous-like pattern (see Fig. 3) with a well-defined band centered at about $2\theta = 25°$; this position agree with the ones reported by Valentovic *et al.* [17] for amorphous CdTe, and by Alvarez-F. *et al.* [18] for amorphous $Cd_{0.95}Fe_{0.05}Te$ thin films. From the XRD patterns in Fig. 3 we observe that the main effect of the high Sb

TABLE I. Calculated lattice parameters values based on the cubic indexing for the different CdSbTe thin films, with Sb concentration varying in the range 8–60 at %. The CdTe single-crystal value for the lattice parameter as taken from the ASTM X-ray powder data file is $a = 6.481$ Å.

Sample	Nominal Film	Structure	Lattice Parameter a (Å)	hk1
A_0	CdTe	Cubic	6.497	111
A_1	$Cd_{0.96}Sb_{0.08}Te_{0.96}$	Cubic	6.510	111
A_2	$Cd_{0.95}Sb_{0.10}Te_{0.95}$	Cubic	6.511	111
A_3	$Cd_{0.94}Sb_{0.12}Te_{0.94}$	Cubic	6.514	111
A_4	$Cd_{0.85}Sb_{0.30}Te_{0.85}$	Amorphous	—	—
A_5	$Cd_{0.75}Sb_{0.50}Te_{0.75}$	Amorphous	—	—
A_6	$Cd_{0.70}Sb_{0.60}Te_{0.70}$	Amorphous	—	—

concentration in the A_4, A_5 and A_6 samples consists in the amorphization of the crystalline structure.

3.3. Room-temperature resistivity measurements

In Fig. 4 it is shown the dependence of the room temperature resistivity on the Sb concentration. The A_0 sample was found to be insulating ($\rho = 9.8 \times 10^8$ Ω–cm), and it is a typical result for this type of compounds [19]. The A_1, A_2 and A_3 samples showed resistivities around three orders of magnitude lower, indicating that some part of the Sb concentrations is effectively doping the sample. Due to self-compensation problems for II-VI compounds [19,2], the amount of Sb which is really doping the film has not been determined because we have experienced considerable difficulties in the Seebeck and Hall measurements. However, it has been shown by Bicknell, Giles and Schetzina [21] that under special conditions Sb can really substitutionally dope CdTe layers without self-compensation problems.

The resistivity of the A_4 sample increases in relation to the ones for the A_1–A_3 films, reflecting the structural amorphization of the film. For samples A_5 and A_6 the resistivity values drop to values between 10^2 and 10^4 Ω–cm as a result of the very high Sb concentration, which can result in impurity conduction like in Sb-doped a-Ge and a-Si [22] and Ge_xSe_{1-x} amorphous thin films [23].

3.4. Conductivity versus temperature

The electrical conductivity as a function of the temperature produces a linear relationship in an Arrhenius type plot [18], showing a single well-defined activation energy, E_a, in the temperature range (25–150 °C) analyzed; this is an evidence of thermally activated process for the electrical conduction in the polycrystalline samples, and of a thermally activated conductivity process in extended states for the amorphous samples of the form $\sigma = C\exp(-E_a/kT)$, where E_a is the thermal activation energy for the conduction process, k is the Boltzmann's constant, and $C = \sigma_0 \exp(\beta/k)$, with σ_0 a parameter related to the mobility and the density of states, and β the temperature coefficient [22–25].

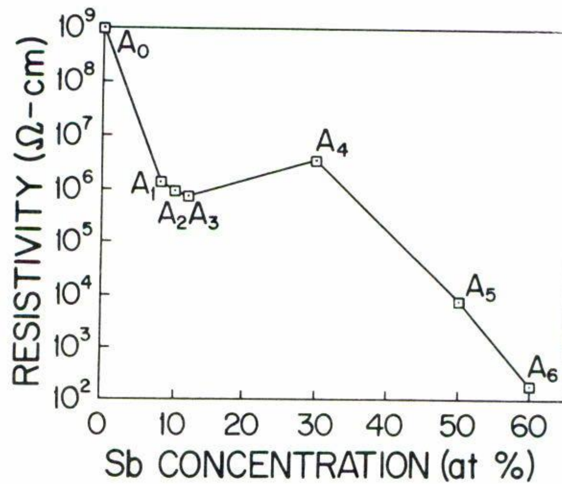

FIGURE 4. Dependence of the room temperature resistivity for the CdSbTe films as a function of a the Sb content. A variation of almost seven orders of magnitude is observed between the resistivity value for the CdTe film, and the value for the films with the highest Sb content.

The activation energies for the conductivity process as a function of the Sb concentration, and the C_i's values for the amorphous films are shown in Fig. 5. The activation energy value for the CdTe film ($E_a = 0.67$ eV) is an indication of an intrinsic conduction process. The marked increase in the electrical conductivity when the Sb concentration increases from zero to 10% (see Fig. 4) is mainly caused by a reduction of the activation energy (~ 0.34 eV) reflecting that Sb is effectively doping the samples A_1 and A_2. For sample A_3 an increase in the E_a-value of around 0.1 eV is observed; such increase could be due to a scattering mechanism either via the Sb impurity atoms at that temperature range, and/or via grain boundaries with different potential barriers heights and defect states with respect to those of A_1 and A_2 [26,27].

For amorphous samples, the activation energy E_a decreases from 0.48 eV to 0.24 eV with C-values of around 10–100 Ω^{-1}-cm^{-1}, as the amount of Sb increases. Also, the resistivity drops from 10^6 Ω-cm to about 100 Ω-cm as the Sb concentration increases from 30 to 60%. A similar behavior has been reported for some other amorphous materials [28–30]. In those studies, the compositional and/or doping impurity effects on the amorphous thin film conductivity were interpreted as due to an extensive participation of localized states near the mobility edges in the conduction process at room temperature, and/or as an effect of the impurities on the extended states with an activated mobility. From the magnitude of the C_i values, the decreases in E_a and the high Sb content, we suppose that an extensive participation in the conduction process of localized states near the mobility edges, is the more feasible explanation to our results; however, more extensive studies are needed to give a definitive conclusion.

A detailed study on the film growth, structure and bandgap energies as a function of the substrate temperature ($\sim$ 50–250 °C) for different Sb concentration (0–60%) is being carried out and will be published elsewhere.

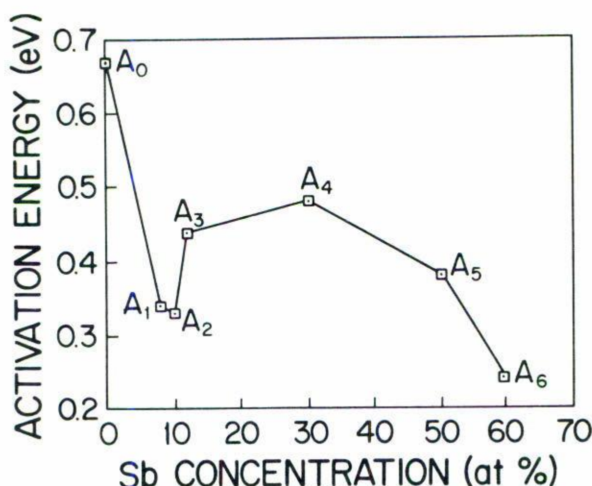

FIGURE 5. Variation of the activation energy for the conductivity process in terms of the Sb concentration in the films. The activation energies were obtained from an Arrhenius-type plot of the resistivity versus temperature in the range 25–150 °C. The C_i values 4.5×10^1, 3.2×10^2 and 7.3×10^1 Ω^{-1} correspond to A_4, A_5, A_6 samples respectively.

4. CONCLUSIONS

In summary, we have presented here the initial results on the structure, composition and electrical properties of CdSbTe thin films and its dependence on the Sb concentration for values in the range 0–60%.

From AES quantitative analysis we have shown the amphoteric behavior of Sb atoms in substituting in nearly equal proportions the Cd and Te atoms in the CdTe lattice. Using X-ray diffractometry we found that for Sb concentrations up to around 12%, the films are polycrystalline, growing in the cubic phase with a strong (111) preferential orientation; and also that the microcrystalline grain size is around 200–300 Å. For the high values of Sb concentration, films show an amorphous-like XRD pattern evidencing that the effect of the high Sb content is in the amorphization of the CdTe lattice.

Finally, the electrical resistivity measurements at room temperature and as a function of the sample temperature showed that for low x–values part of the Sb concentration goes in doping the film; and that for the amorphous films with the highest Sb content an impurity conduction mechanism is responsible for the drop in the resistivity down to values of ~ 100 Ω–cm. The activation energies for the conductivity process decreases for films with low Sb content reflecting the doping by Sb atoms; and goes down even more for the films with high Sb concentration, probably due to a participation in the conduction process of localized states near the mobility edges.

ACKNOWLEDGEMENTS

We thank to Dra. Leticia Baños from IIM-UNAM for her very helpful assistance in the X-ray measurements. We acknowledge the partial financial support from CONA-CYT/México, and the Organization of American States.

REFERENCES

1. B. Pamplin, T. Kiyosawa and K. Masumoto, *Prog. Cryst. Growth and Charact.* **1** (1979) 331.
2. A.L. Gentile, *Prog. Cryst. Growth and Charact.* **10** (1984) 241.
3. R.G. Goodchild, O.H. Gughes, S.A. López-Rivera and J.C. Woolley, *Can. J. Phys.* **60** (1982) 1096.
4. A. Miller, A. MacKinnon and D. Weaire, *Solid State Physics* **36** (1981) 119.
5. S.A. López-Rivera, L. Martínez, J.M. Briceño-Velasco, R. Echeverría and G. González de Armengoll, *Prog. Cryst. Growth and Charact.* **10** (1984) 297.
6. W.R. Runyam, in *Semiconductor Measurement and Instrumentation*, McGraw Hill (1975), p. 67.
7. O. Zelaya, F. Sánchez-Sinencio, J. González-Hernández, J.L. Peña, M. Farias, L. Cota-Araiza, G.A. Hirata and F. Rábago, *J. Vac. Sci. Technol.* **A7** (1989) 245.
8. R.D. Feldman, R.L. Opila and P.M.B. Bridenbaugh, *J. Vac. Sci. Technol.* **A3** (1985) 1988.
9. H.L. Hwang, C.M. Fon, S. Shea, V. Dalton, M.H. Yang and C.S. Shen, *Prog. Cryst. Growth and Charact.* **10** (1984) 175.
10. O. Alvarez-Fregoso, J.G. Mendoza-Alvarez, F. Sánchez-Sinencio and A. Huanosta, *J. Appl. Phys.* **64** (1988) 3928.
11. A. Russak, *J. Vac. Sci. Technol.* **A3** (1985) 433.
12. O. Alvarez-Fregoso, J.G. Mendoza-Alvarez and F. Sánchez-Sinencio, *Lectures on Surface Science*, Eds. G.R. Castro and M. Cardona, Springer Series (1987) p. 52.
13. I. Hernández-Calderón, J.L. Peña and S. Romero, *Lectures on Surface Science*, Eds. G.R. Castro and M. Cardona, Springer Series (1987) p. 56.
14. F. Chwang, J. Smith and R. Crowell, *Solid State Electron.* **17** (1974) 1217.
15. G. Hodes, J. Manassen, S. Neagi, D. Cahen and Y. Mirosvsky, *Thin Solid Films* **90** (1982) 433.
16. D. Culity, in *Elements of X-ray Diffraction*, Addison-Wesley, New York (1956).
17. D. Valentovic, J. Cervenak, S. Luby, M.L. Aldea and T. Botila, *Phys. Status Solidi* **A56** (1979) 342.
18. O. Alvarez-F., J.G. Mendoza-Alvarez, F. Sánchez-Sinencio, S. Romero and M.A. Vidal, *J. Vac. Sci. Technol.* **A5** (1987) 1798.
19. K. Zanio, in *Semiconductors and Semimetals*, Vol. 13, Academic Press, New York (1978).
20. R.N. Bicknell, N.C. Giles and J.F. Schetzina, *Appl. Phys. Lett.* **49** (1986) 1095.
21. R.N. Bicknell, N.C. Giles and J.F. Schetzina, *Appl. Phys. Lett.* **49** (1986) 1735.
22. N. Van Dong and T.Q. Hai, *J. Non-Cryst. Solid* **35-36** (1980) 351.
23. T. Tri Nang, M. Okuda, T. Matsushita, S. Yokuta and A. Susuki, *Jap. J. Appl. Phys.* **15** (1976) 849.
24. P.K. Baht, K.L. Bhatia and S.C. Katyal, *J. Non-Cryst. Solid* **27** (1978) 399.
25. N.F. Mott and E.A. Davis, in *Electronic Processes in Non Crystalline Solids*, Clarendon Press, Oxford (1971) p. 339.
26. T.L. Kamins, *J. Appl. Phys.* **42** (1971) 4357.
27. J.Y.W. Seto, *J. Appl. Phys.* **46** (1975) 5247.
28. P. Nagels, M. Rotti and S. Vikhrov, *J. Phys. Colloque C4* Supp. No. 10 **42** (1981) 907.
29. C. Wood, L.R. Gilbert, R. Mueller and C.M. Garner, *J. Vac. Sci. Technol.* **10** (1973) 739.
30. N.F. Mott, *Phil. Mag* **37** (1978) 127.